ISSN 1349-1148
JAXA-RR-03-017E

JAXA Research and Development Report

Unsteady Shock Wave Motions on a Thin Airfoil at Transonic Speeds Caused by Aileron Oscillations

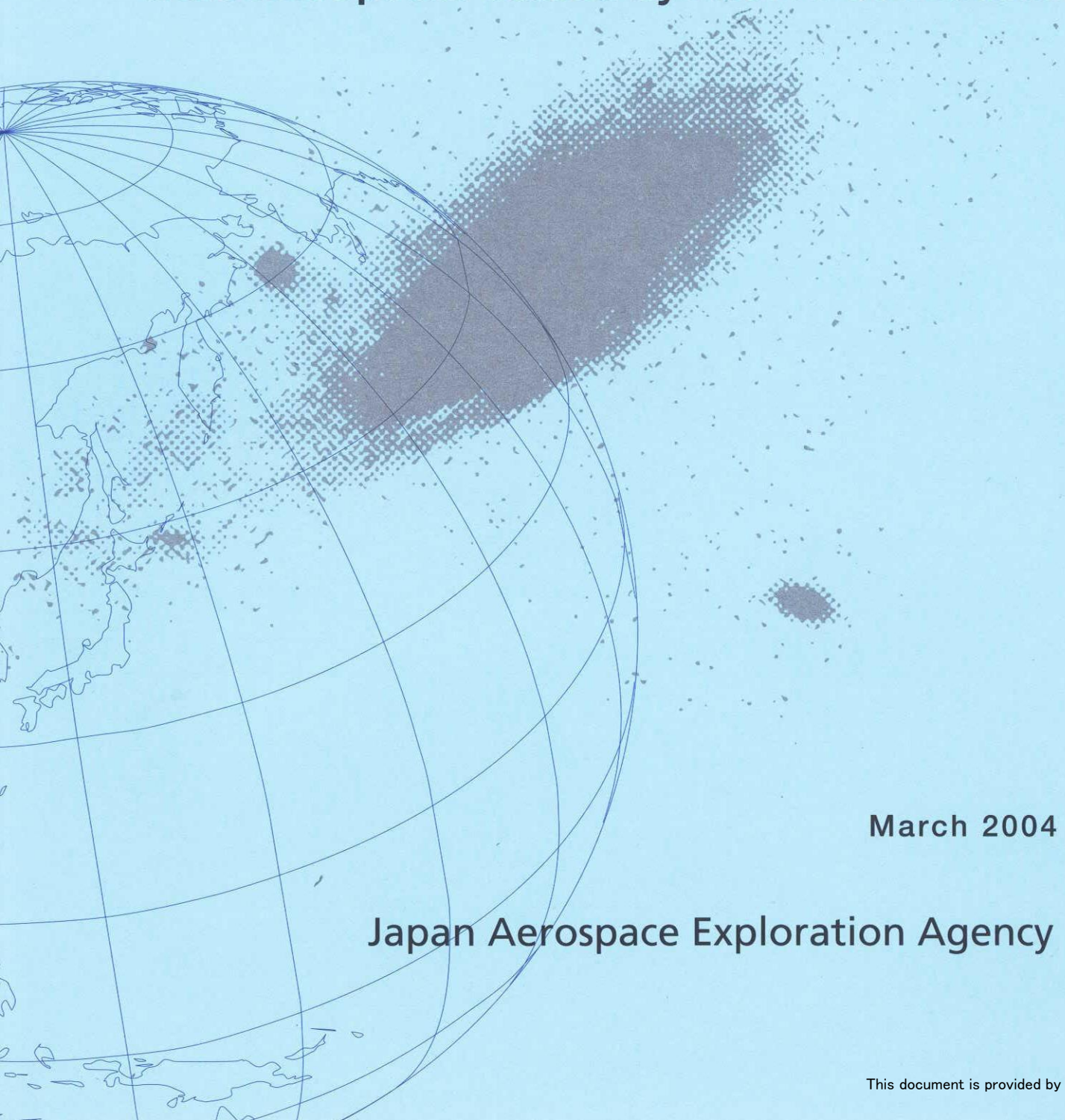

March 2004

Japan Aerospace Exploration Agency

JAXA-RR-03-017E

JAXA Research and Development Report
宇宙航空研究開発機構研究開発報告

Unsteady Shock Wave Motions on a Thin Airfoil at Transonic Speeds Caused by Aileron Oscillations

遷音速における薄翼上衝撃波のエルロン振動による非定常挙動について

Masato TAMAYAMA , Jiro NAKAMICHI
玉山　雅人、中道　二郎

Structure Research Group
Institute of Space Technology and Aeronautics
総合技術研究本部 構造解析研究グループ

March 2004
2004年3月

Japan Aerospace Exploration Agency
宇宙航空研究開発機構

Unsteady Shock Wave Motions on a Thin Airfoil at Transonic Speeds Caused by Aileron Oscillations*

Masato TAMAYAMA[*1], Jiro NAKAMICHI[*1]

Abstract

Aileron buzz is one of the most dangerous phenomena encountered in high-speed flight. If the wing is thin, conventional aileron buzz, which is always accompanied by boundary layer separation, will not occur. In this case, shock wave motions are of great importance in the aileron buzz phenomenon. To acquire fundamental knowledge on this type of aileron buzz, the relationship between shock wave movement and aileron hinge moment have been studied with numerical simulations. A forced aileron oscillation was applied to the unsteady Navier-Stokes simulations around a two-dimensional NACA0003 airfoil with 25% chord-length aileron at the trailing edge. In this study, the Mach number, airfoil angle of attack and amplitude and reduced frequency of aileron oscillation were varied. The influence of these parameters on the flow characteristics is described, taking into account the shock wave motions on the aileron surface and the aileron hinge moment. It is observed that, if the shock wave exists on the aileron, it oscillates around a position located upstream of the steady shock wave. The position of a shock wave moving on the aileron is greatly influenced by flow viscosity. It is also observed that the shock wave oscillates non-harmonically, even though the aileron oscillates harmonically. This characteristic was studied by simulating the shock wave motion, assuming a one-dimensional flow field. From this simulation, it is observed that the pressure ratio across a shock wave changes non-harmonically and the shock wave moves non-harmonically.

Key words: Transonic Flow, Thin Airfoil, Unsteady Aerodynamics, Shock Wave, Aileron Buzz

概　　要

航空機のエルロン・バズは高速飛行において非常に危険な現象である。特に薄翼の航空機では、衝撃波による境界層はく離の発生が抑えられる結果、翼面での衝撃波振動自体がエルロン・バズの発生に直接結びつき、急速にエルロン振動が成長する。このようなエルロン・バズ現象に対する情報は薄翼航空機の存在が少ないため非常に少ない。一方、超音速旅客機の様な高速で飛行する航空機ではこのエルロン・バズの検討が必須となるため、将来の先進的高速航空機開発に対するデータ蓄積のため同エルロン・バズ現象の検討を行う必要がある。この必要性のもと、翼弦長の25%の長さのエルロンを持つNACA0003翼に対し、エルロンに強制的な振動を与えた場合の衝撃波の振動とエルロンに働くモーメントの関係について検討を進めた。本研究では、マッハ数、翼の迎角、及び、エルロン振動の振幅と振動数を変化させ、翼周りの流れに対するこれらの影響、及び、エルロンに働く非定常モーメントとの関係を、流体力学シミュレーション技術を用いて調べた。この結果、衝撃波が定常衝撃波位置に比べて上流側で振動する現象が見られ、これには粘性が強く影響していることが判明した。また、エルロン舵角を調和振動的に変化させても、衝撃波の位置は調和振動的にならないことが観察され、これには衝撃波前後の圧力比が調和振動的に変化しないことが影響していると考えられた。以上、エルロン・バズ発生に直接関係する衝撃波の運動は、単純な線形空気力学では扱えない要素を含んでいることが明らかとなった。

* received 10 February, 2004（平成16年2月10日受付）

*1 Structure Reseach Group, Institute of Space Technology and Aeronautics
（総合技術研究本部　構造解析研究グループ）

1 INTRODUCTION

Aileron buzz is an aeroelastic phenomenon that appears at the speed equal to or faster than the transonic speed. It is categorized into three regions, A, B and C[1]. Region A buzz occurs if the flow separates from a wing as a result of a strong interaction between a shock wave and a boundary layer, and the separated flow oscillates unsteadily. Region A buzz has been studied precisely by some researchers[1),2)] because the flow field relating this buzz can be occurred on conventional transonic airplanes. Region C buzz occurs when a shock wave appears at the aileron trailing edge. The flow field constituting Region C buzz is a supersonic potential flow and, therefore, the prediction of its occurrence will be done relatively with ease. Region B buzz can be caused only by an existence of shock waves oscillating on an aileron[3)]. Our study originates from the development of Japanese non-powered *N*ational *EX*perimental airplane for next generation *S*upersonic *T*ransport, *NEXST-1*. Even though the NEXST-1 was designed to be free from aeroelastic phenomena during the flight envelope, the severest aeroelasticity phenomenon was an aileron buzz at transonic speeds[4)]. The NEXST-1 has a thin and warped wing, and, therefore, a shock wave / boundary layer separation is not easily generated. Aileron buzz in the NEXST-1 development had to be Region B buzz. This type of buzz will grow rapidly[5)]. It is difficult to alleviate Region B buzz with augmenting structural rigidity for airplanes like NEXST- 1, because these airplanes do not have an extra space inside their thin wings. As to active control technologies, before selecting the effective controlling method, one needs to consider detailed information about the flow field relating Region B buzz. This means that one needs to prepare information about the relations among aileron oscillations, unsteady shock wave motions, and resulting aerodynamic moment loaded on the aileron hinge.

Tamayama, *et al.* presented the above information acquired from the two-dimensional Navier-Stokes simulations around an NACA0003 airfoil with an aileron under forced oscillations[3)] and described the influence of the free-stream Mach number, which corresponded to the influence of the shock wave positions. In the present study, we expand the considerations to the influences of the wing angle of attack and the amplitude and reduced frequency of the aileron oscillations.

In our study, it was observed that, if the shock wave existed on the aileron, it oscillated around the position which located upstream of the steady shock wave. This inconsistency has great importance when the unsteady aerodynamic forces are estimated with a simple model, which assumes shock waves oscillating around the steady shock wave positions. One of the most serious influences caused by this inconsistency can be seen when the pressure distributions are acquired experimentally. We may not average the unsteady pressure distributions in order to acquire the steady pressure distributions. It is made clear in this paper that the inconsistency of shock wave positions between steady and unsteady flow fields is greatly influenced by the nature of viscous flow.

It was also observed that the shock wave oscillated non-harmonically even though the aileron oscillated harmonically. This influences on the linear simulations, which usually assume the shock wave harmonic motions. In order to clear the fundamental cause of this phenomenon, the shock wave motion was simulated by assuming a simple one-dimensional flow field on the aileron. The flow upstream of the shock wave was assumed as a potential flow generated by a dynamic aileron motion. The flow downstream of the shock wave was assumed to follow the unsteady pressure distribution same as one simulated for the flow without shock waves. Even from this simple simulation, the non-harmonic shock wave motion was reproduced, that means, the shock wave stayed for a longer period in the downstream half cycle than the upstream half cycle. The reason to cause the non-harmonic shock wave motion can come from the fact that the pressure ratio across the shock wave is not harmonic if the shock wave oscillates on the aileron.

2 SIMULATIONS

2.1 Method

The CFD code developed by Kheirandish, *et al.*[6)] is used in this study. Two-dimensional Navier-Stokes

equations are analyzed. The thin-Layer assumption is used for the boundary layer. The turbulent model is the Baldwin-Lomax model[7] under the assumption of no large-scale boundary layer separation. The Yee-Harten TVD (Total Variation Diminishing) method[8] is used as a scheme. The equations are analyzed with ADI (Alternating Direction Implicit) method. After acquiring the steady flow field, the unsteady flow is calculated in a time accurate manner with an appropriate time step by applying a harmonic oscillation of aileron deflection angle. At each time step, a set of governing equations is solved. The validation of this code was confirmed in Ref.3 by proving enough reliability in estimating shock waves.

A NACA0003 airfoil with an aileron was simulated in this study. The Aileron has a 25% chord length and it is installed at its trailing edge area. C-type grids, which sizes are 189x80 and 237x80, are used. The latter grid is used for the cases with a high angle of attack. The former grid is shown in Fig.1. c is the airfoil chord length.

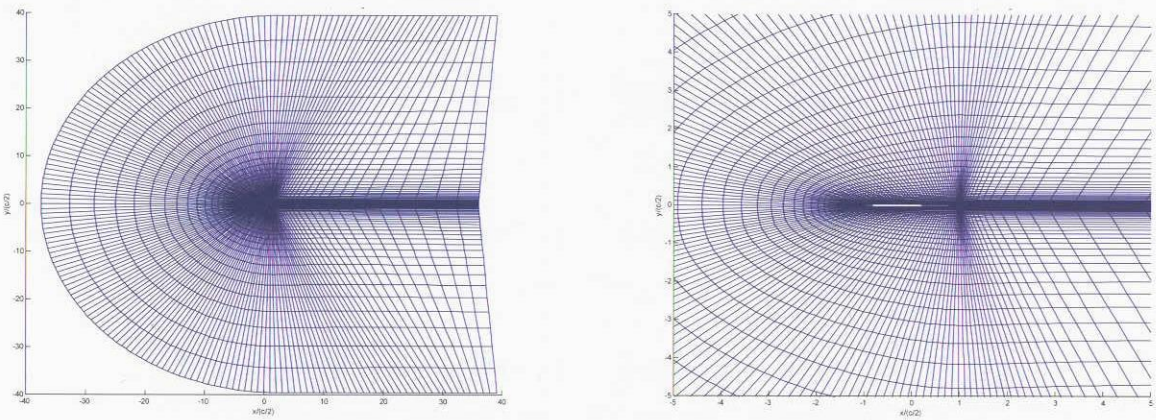

(a) Whole View (b) Close View

Figure 1 Computational Grid (C type, 189x80, NACA0003)

Table 1 Simulated Cases

$Re = 1.0 \times 10^7$

	k = 0.05	k = 0.20	k = 1.00	k = 2.00
$\delta_{amp} = 0.5^\circ$		$\alpha=0^\circ, 2^\circ$		
$\delta_{amp} = 1.0^\circ$		$\alpha=0^\circ,2^\circ$		
$\delta_{amp} = 2.0^\circ$	$\alpha=0^\circ,2^\circ$	$\alpha=0^\circ, 1^\circ, 2^\circ, 4^\circ$	$\alpha=0^\circ, 2^\circ$	$\alpha=0^\circ, 2^\circ$
$\delta_{amp} = 4.0^\circ$		$\alpha=0^\circ, 2^\circ$		

α	0°	1°	2°	4°
M	0.800, 0.920, 0.935, 0.942, 0.950	0.890, 0.900, 0.910, 0.920, 0.930, 0.940	0.860, 0.870, 0.880, 0.890, 0.900, 0.920	0.820, 0.840, 0.850, 0.860, 0.880

2.2 Cases

Table 1 shows the simulated cases; where the angle of attack, α, the amplitude, δ_{amp} , and the reduced frequency, $k=\pi fc/U_{inf}$, of the aileron oscillation and the free-stream Mach number, M_{inf}, were varied. The aileron deflection angle, δ, is defined as positive if the aileron stays downward. The Reynolds number, Re ($=\rho_{inf}U_{inf}c/\mu$), was set to the fixed value, $1.0\text{x}10^7$, for every case. Here, f is the frequency of the aileron oscillation; U_{inf} is the free-stream velocity; ρ_{inf} is the free-stream air density; μ is the viscosity. In the simulated results, the cases for $\delta_{amp}=2^\circ$ and $k=0.2$ are taken as the reference cases. In the next section, the considerations are given by comparing results with this reference cases.

3 CONSIDERATIONS

3.1 Influences of Parameters

[Influence of Angle of Attack]First, it is described how the angle of attack, α, influences on the flow field and the aileron hinge moment. Figure 2 shows the C_p contours with time varying. C_p is the pressure coefficient defined as follows:

$$C_p = \frac{P - P_s}{q} \tag{1}$$

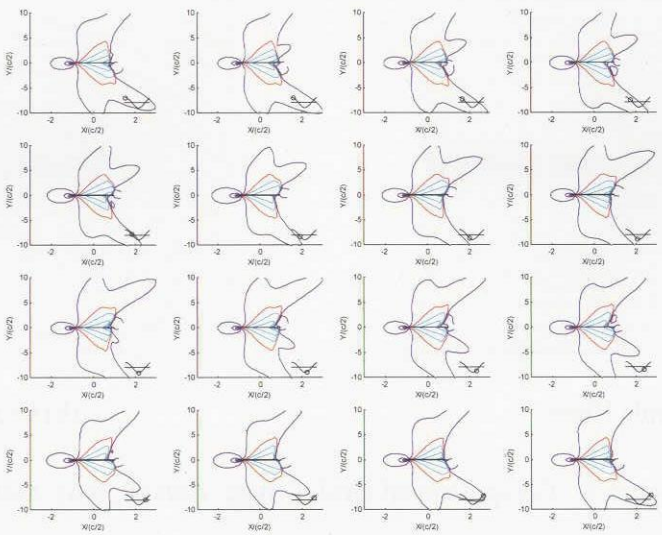

(a) $\alpha=0^\circ$, $M_{inf}=0.942$

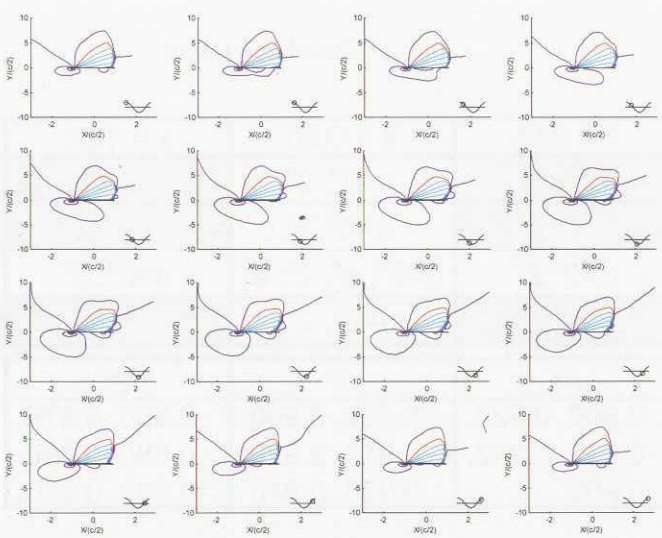

(b) $\alpha=2^\circ$, $M_{inf}=0.890$

Figure 2 Pressure Coefficient Contours ($\delta_{amp}=2^\circ$, $k=0.20$)

Here, P is the local static pressure; P_s is the free-stream static pressure; q is the free-stream dynamic pressure. The case presented in Fig. 2(a) is for α=0°, δ_{amp}=2°, k=0.20 and M_{inf}=0.942. The aileron deflection is indicated as a curve with a small circle shown at the right below corner. The blue, pale-blue and red curves show the contours at subsonic, supersonic and sonic speeds, respectively. At the case of α=0°, the flow field changes with a half cycle phase difference between the upper and lower surfaces. Figure 2(b) shows the case for α=2°, δ_{amp}=2°, k=0.20 and M_{inf}=0.890. At this condition, the supersonic region appears only on the upper surface.

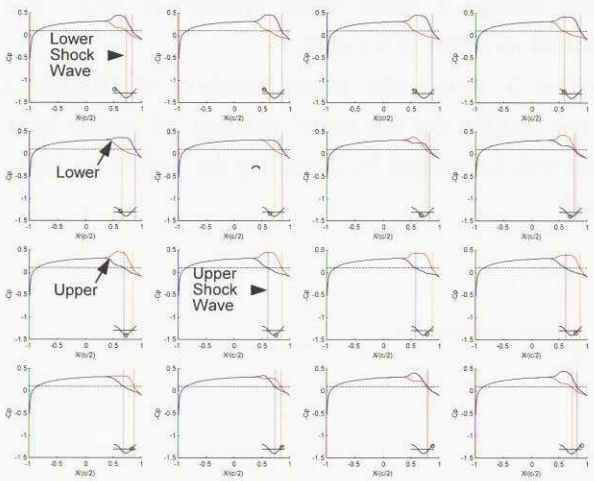

(a) α=0°, M_{inf}=0.942

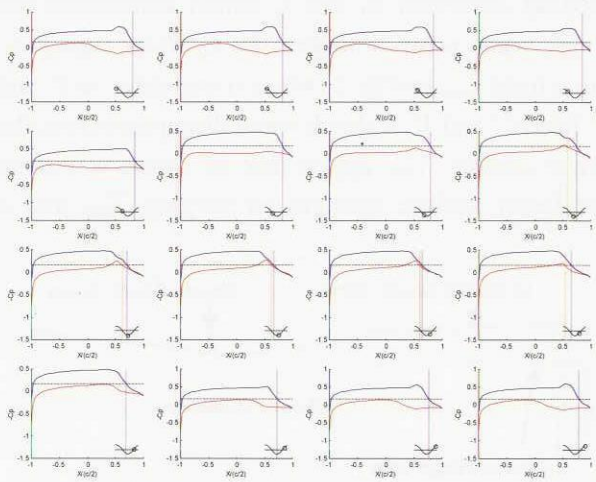

(b) α=1°, M_{inf}=0.910

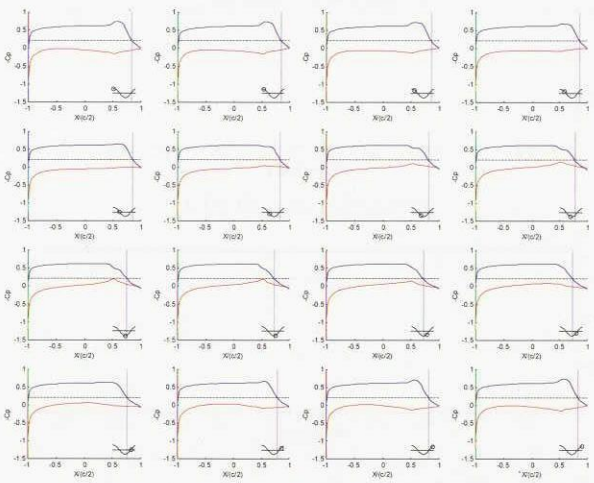

(c) α=2°, M_{inf}=0.890

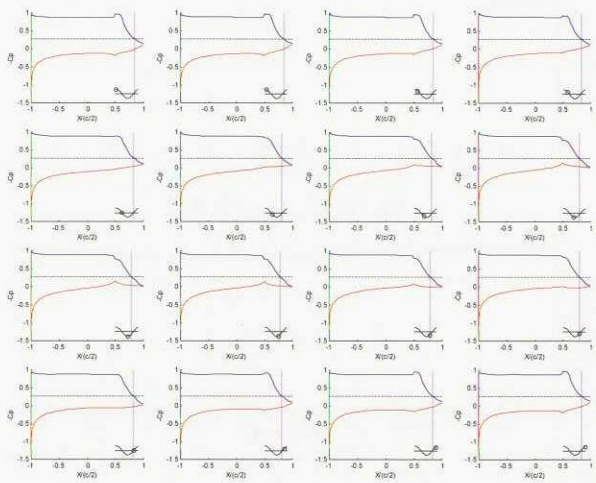

(d) α=4°, M_{inf}=0.860

Figure 3 Pressure Coefficient Distributions (δ_{amp}=2°, k=0.20)

Figure 3 shows the C_p distributions on the airfoil surfaces with time varying. M_{inf} for each α case is selected so that the shock wave oscillates almost at the same position on the aileron upper surface. The solid blue curve shows the distribution on the upper surface and the solid red one on the lower surface. The blue dashed-line shows the position of the shock wave on the upper surface and the red one on the lower surface. The chain-line means the critical C_p value. The shock wave position is defined by the method described in Ref.3, which determines the shock wave position where the C_p value equals to the critical C_p. In Fig. 3, when α increases to 2° and 4° from 0° and 1°, a shock wave disappears from the lower surface. The appearance of shock waves on the lower surface changes as varying δ_{amp} and k values.

According to the above criterion to determine a shock wave position, the history of shock wave motion was drawn as Fig. 4. The magenta line shows the aileron motion and dose not indicate the absolute value but only the phase change. Although, for every case, the steady shock wave stays at almost the same position on the upper surface, the amplitude of the shock wave motion decreases as α increases. As to the shock waves on the lower surface, even though a shock wave appears at α=1°, it is limited to a part of a cycle.

Figure 5 shows the mean position of the shock wave motion on the upper surface, of which location was calculated by applying the following equation:

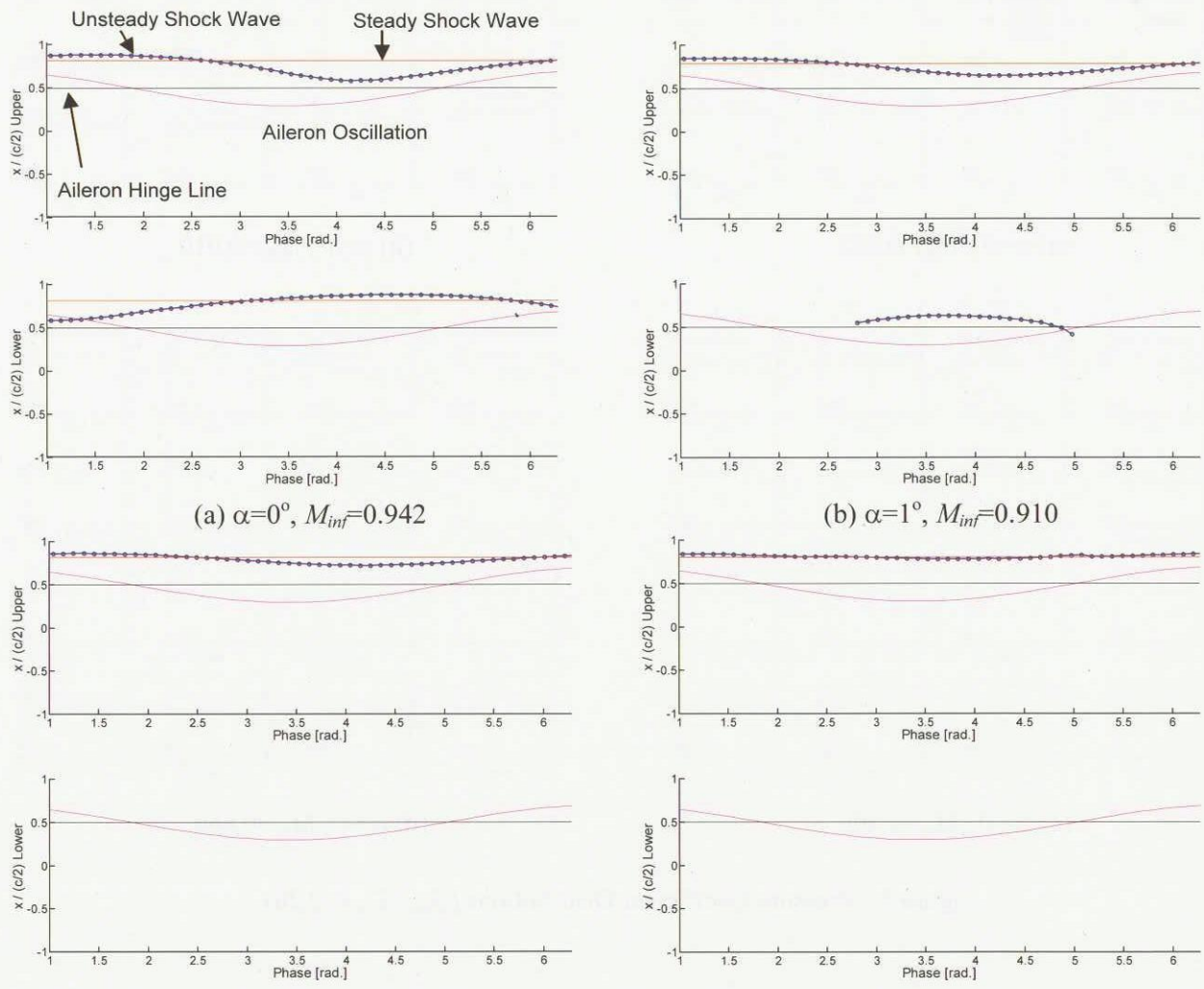

(a) α=0°, M_{inf}=0.942

(b) α=1°, M_{inf}=0.910

(c) α=2°, M_{inf}=0.890

(d) α=4°, M_{inf}=0.860

Figure 4 Time-Histories of Shock Wave Motions (δ_{amp}=2°, k=0.20)

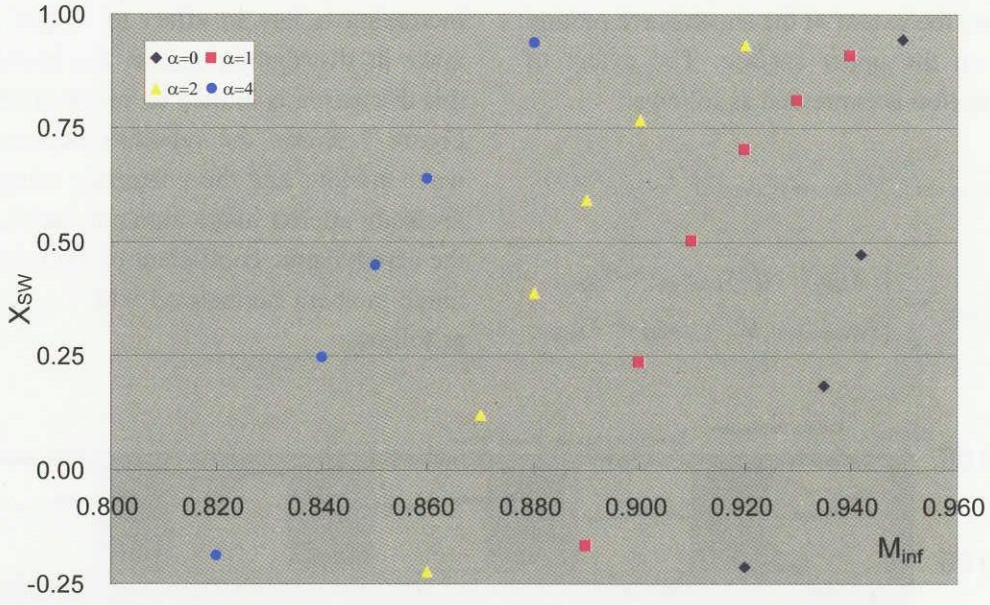

Figure 5 Shock wave Mean Position against M_{inf} (Upper Surface)

$$\left.\begin{aligned} x_{SW} &= \frac{1}{2}\left(x_{Upstream} + x_{Downstream}\right) \\ X_{SW} &= \frac{x_{SW} - x_{Hinge}}{L_{Aileron}} \end{aligned}\right\} \qquad (2)$$

x_{SW}, $x_{Upstream}$ and $x_{Downstream}$ express the mean, the most upstream and the most downstream positions of the shock wave motions, respectively. x_{Hinge} means the location of the aileron hinge, which corresponds to the aileron leading edge in the simulations. x_{SW} is normalized with the aileron chord length, $L_{Aileron}$, and originates from the aileron hinge location. The normalized value is described with the capital letter, X_{SW}. If the same value of X_{SW} is considered for all α cases, M_{inf} corresponding to this X_{SW} decreases as α increases. The change of X_{SW} against M_{inf} shows linearity unless the shock wave moves close to the trailing edge.

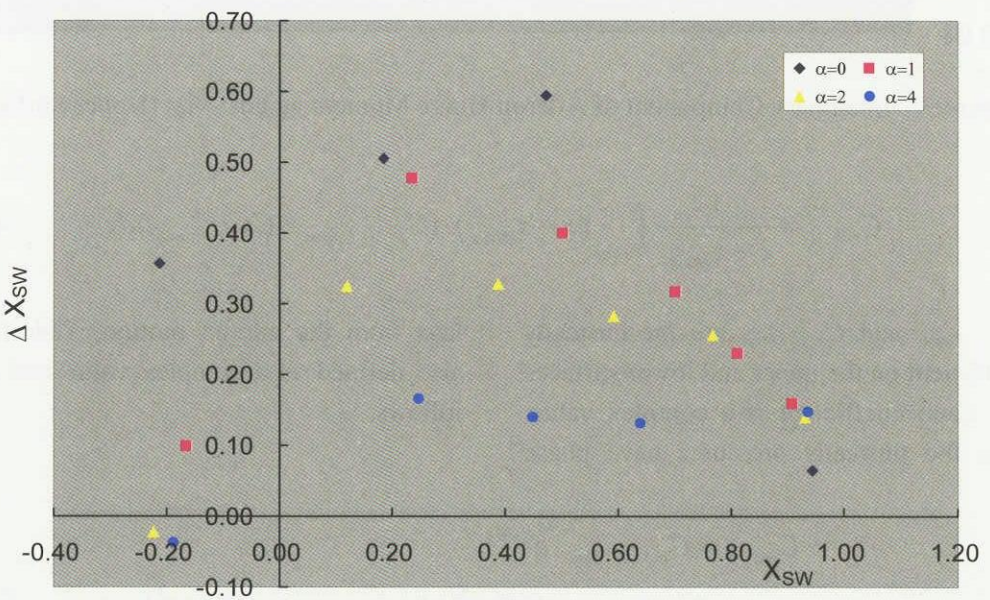

Figure 6 Shock Wave Extent against Shock wave Mean Position (Upper Surface)

Figure 6 shows the extent of the shock wave motion against X_{SW} on the upper surface. The extent of shock wave motion is expressed as follows:

$$\Delta X_{SW} = \left\{ x_{Downstream} - (x_{Upstream}, x_{Hinge}) \right\} / L_{Aileron} \quad (3)$$

$$(x_{Upstream}, x_{Hinge}) = \begin{cases} x_{Hinge} & if\ x_{Upstream} \le x_{Hinge} \\ x_{Upstream} & if\ x_{Upstream} > x_{Hinge} \end{cases}$$

Increasing α has an effect to reduce ΔX_{SW} and to make its distribution against X_{SW} become flat. But, this discussion is limited to the cases being $X_{SW} > 0$. Figure 7 shows the relations between the shock wave motions and the imaginary component of the unsteady aileron hinge moment, Im($C_{m\delta\_u}$). $C_{m\delta\_u}$ is the aerodynamic coefficient of the unsteady aileron hinge moment normalized with $L_{Aileron}$ and defined as follows;

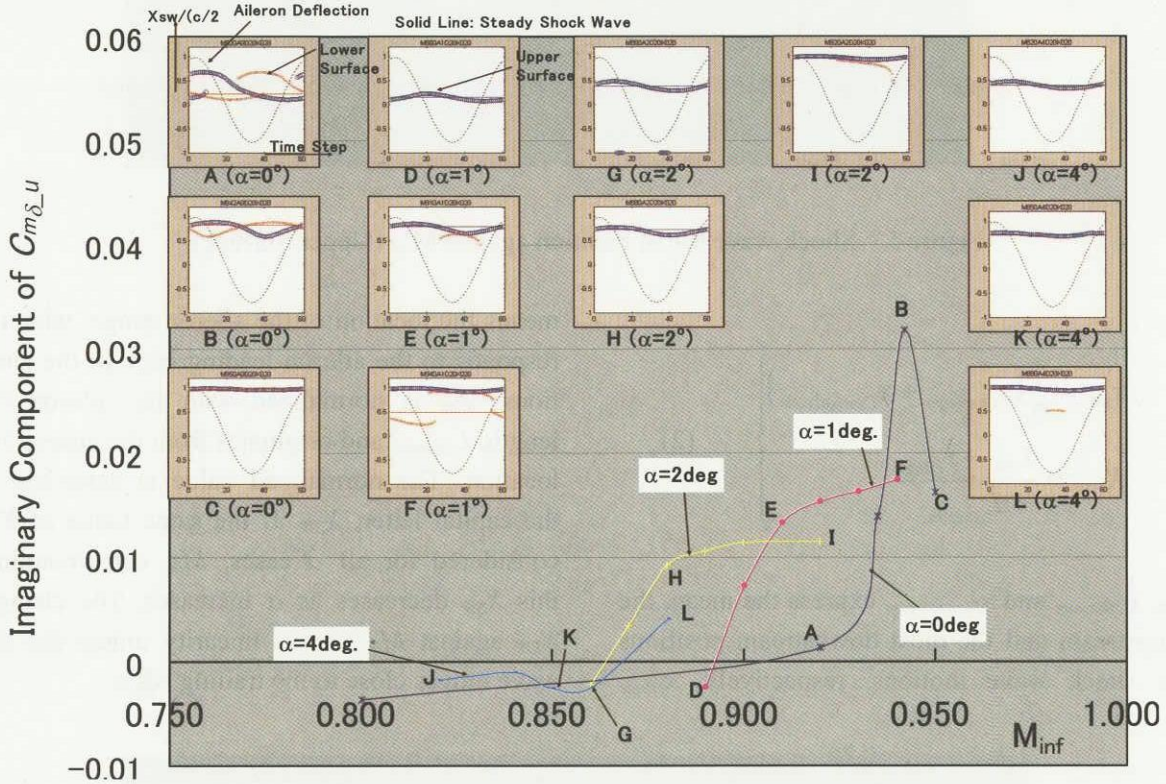

Figure 7 Imaginary Component of Aileron Hinge Moment against M_{inf} (Upper Surface)

$$C_{m\delta\_u} = \frac{1}{c - x_{Hinge}} \int_{x_{Hinge}}^{c} (x - x_{Hinge}) \cdot (C_{P\_u\_Upper} - C_{P\_u\_Lower}) dx \quad (4)$$

Here, $C_{P\_u\_Upper}$ and $C_{P\_u\_Lower}$ are the unsteady pressure coefficient on the upper and lower surfaces, respectively. Each coefficient is a complex value, which means the unsteady pressures have phase lags from the aileron motion. Therefore, $C_{m\delta\_u}$ is also defined as a complex value and described as follows;

$$\begin{aligned} C_{m\delta\_u} &= C_{m\delta\_u\_amp} \cdot e^{i(-\theta)} \\ &= C_{m\delta\_u\_amp} \cdot \cos(-\theta) + i \cdot C_{m\delta\_u\_amp} \cdot \sin(-\theta) \\ &= \mathrm{Re}(C_{m\delta\_u}) + i \cdot \mathrm{Im}(C_{m\delta\_u}) \end{aligned} \quad (5)$$

$$\delta = \delta_{amp} \cdot e^{i2\pi ft} \qquad (6)$$

Here, $C_{m\delta\_u}$ is normalized with the phase of aileron motion. $C_{m\delta\_u\_amp}$ is the amplitude of $C_{m\delta\_u}$ and θ is the phase lag of $C_{m\delta\_u}$ from the aileron motion. Only the first harmonic component of $C_{m\delta\_u}$ is considered here. The black dashed-curve in Fig. 7 expresses the phase change of the aileron motion as same as those shown in Fig. 4. Im($C_{m\delta\_u}$) is an important factor to estimate the state of stability of the aileron motions, which becomes unstable if Im($C_{m\delta\_u}$) goes into a positive value. For the cases of α=0°, Im($C_{m\delta\_u}$) decreases if the shock wave on the upper surface reaches the airfoil trailing edge, but, for the cases of α=1°, 2° and 4°, Im($C_{m\delta\_u}$) does not decrease even if the shock wave reaches the trailing edge. The level that Im($C_{m\delta\_u}$) can reach decreases as α increases. This characteristic is considered to be caused not only by the change of ΔX_{SW} on the upper surface but also by the shock wave formation on the lower surface. In Fig. 7, there also appear shock wave motions on the lower surface, which have a completely different manner from those on the upper surface. The shock wave motion on the upper surface shows a continuous trace for most cases, but the shock wave on the lower surface oscillates intermittently. The duration of the shock wave moving on the aileron lower surface decreases as α increases. This change of the duration time probably influences the reachable Im($C_{m\delta\_u}$) value, and it will be our future work to inspect and to categorize the shock wave motions on the lower surface.

[Influence of Aileron Oscillation Amplitude]

Figure 8 shows ΔX_{SW} against X_{SW} on the upper surface. In Fig.8, the cases for α=0° and 2° are presented. The extent of shock wave motions is broader for α=0° cases than those for α=2°. It is obvious that increasing δ_{amp} has an effect to broaden the extent of shock wave motions. If δ_{amp} is larger than 2°, there appears a certain position where the shock wave oscillates broadest on the upper aileron surface. It is almost the aileron mid-chord.

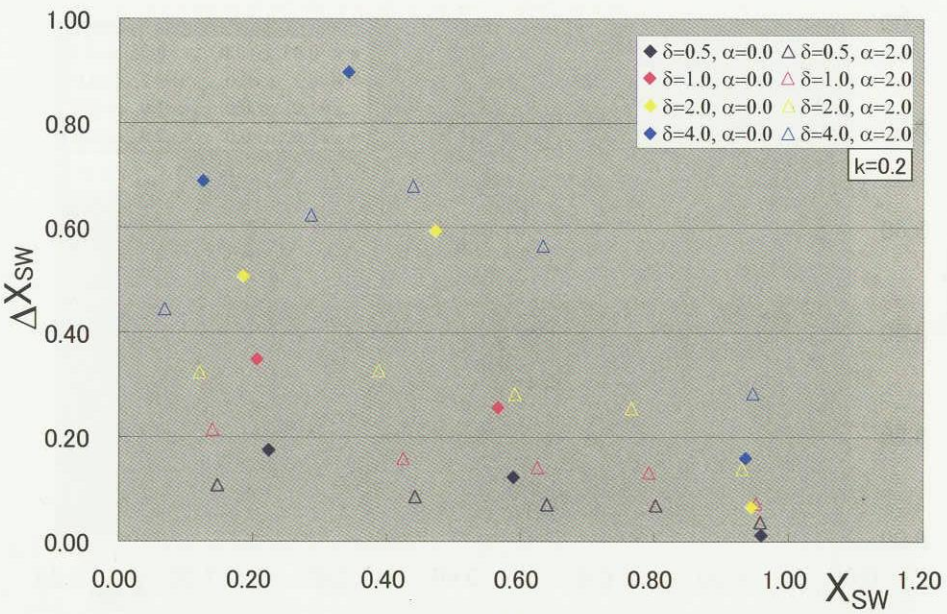

Figure 8 Shock Wave Motion Extent / Influence of δ_{amp} (Upper Surface)

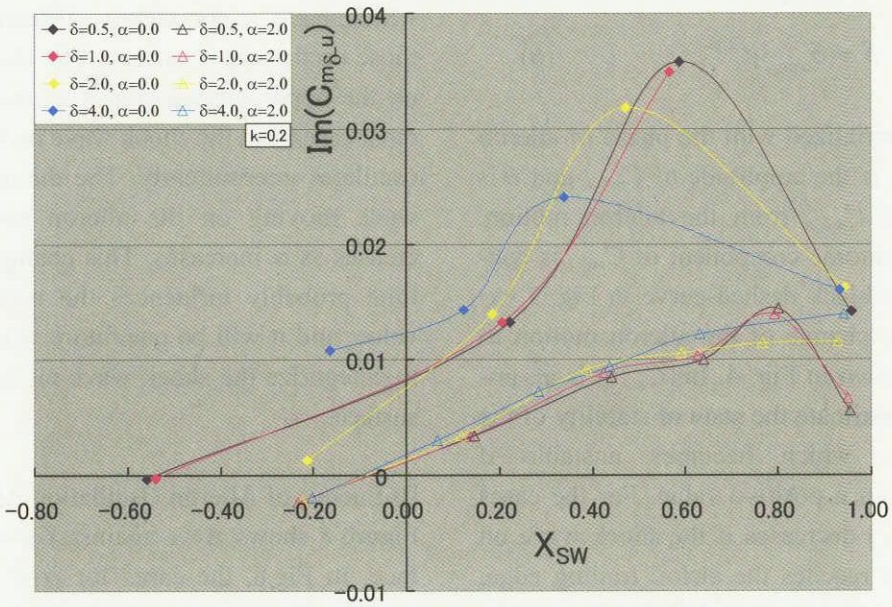

Figure 9 Im($C_{m\delta\_u}$) against X_{SW} / Influence of δ_{amp} (Upper Surface)

Figure 9 shows Im($C_{m\delta\_u}$) distributions against X_{SW}. The Im($C_{m\delta\_u}$) values are normalized by δ_{amp} [degrees]. Changing δ_{amp} influences the Im($C_{m\delta\_u}$) value stronger at α=0° than α=2°. At α=0°, the value that Im($C_{m\delta\_u}$) can reach decreases as δ_{amp} increases. X_{SW} corresponding to the maximum Im($C_{m\delta\_u}$) moves upstream as δ_{amp} increases. On the other hand, for the cases at α=2°, the Im($C_{m\delta\_u}$) variation caused by δ_{amp} difference is not large comparing with those at the α=0° cases.

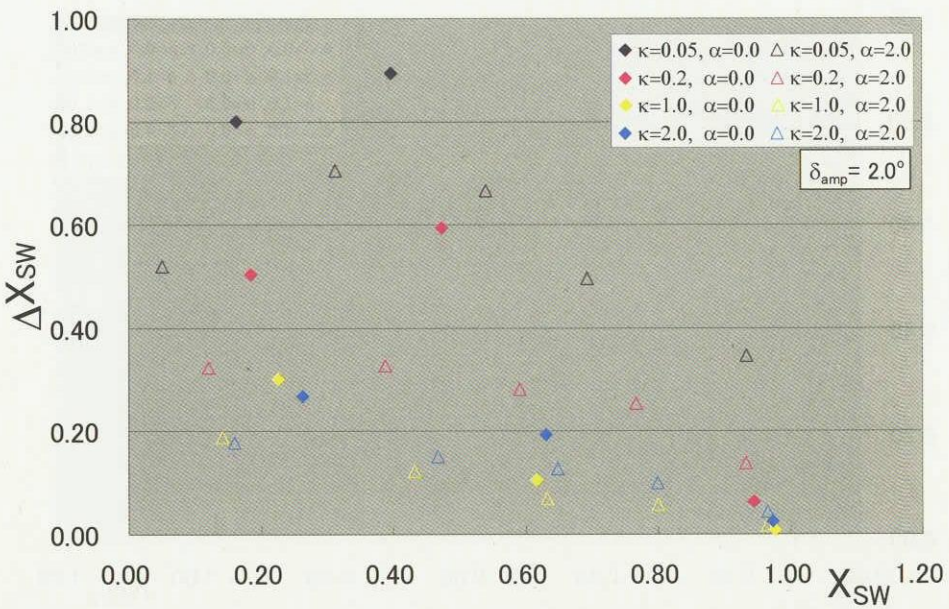

Figure 10 Shock Wave Motion Extent / Influence of k (Upper Surface)

[Influence of Reduced Frequency of Aileron Oscillation]

Figure 10 shows ΔX_{SW} against X_{SW} on the upper surface with k variation. The cases for α=0° and 2° are presented. Increasing k has an effect to reduce ΔX_{SW}. The shock wave oscillates broader at α=0° than α=2° if k is a same value.

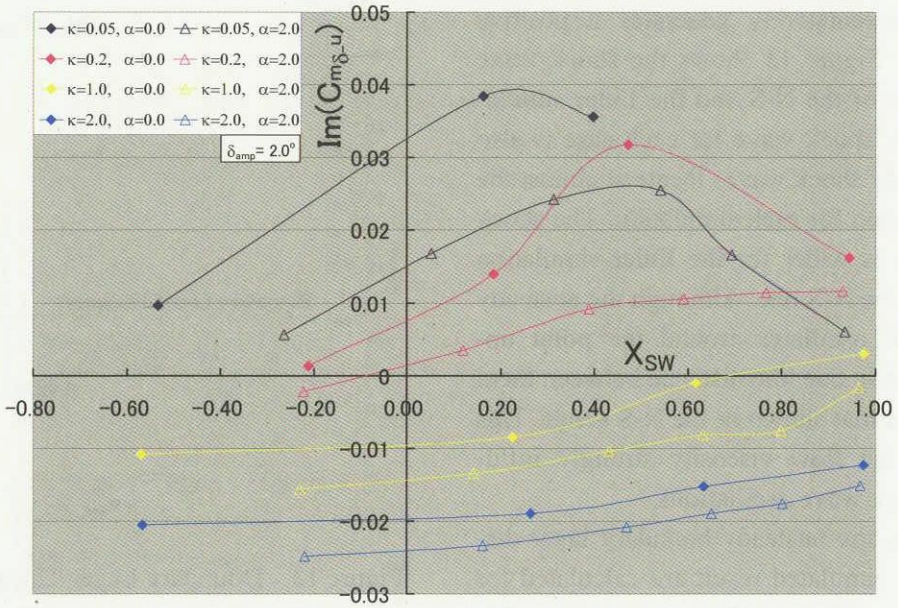

Figure 11 Im($C_{m\delta\_u}$) against X_{SW} / Influence of k (Upper Surface)

Figure 11 shows Im($C_{m\delta\_u}$) values for a unit δ_{amp} [degree] against X_{SW}. Increasing k has an effect to make Im($C_{m\delta\_u}$) decrease its value.

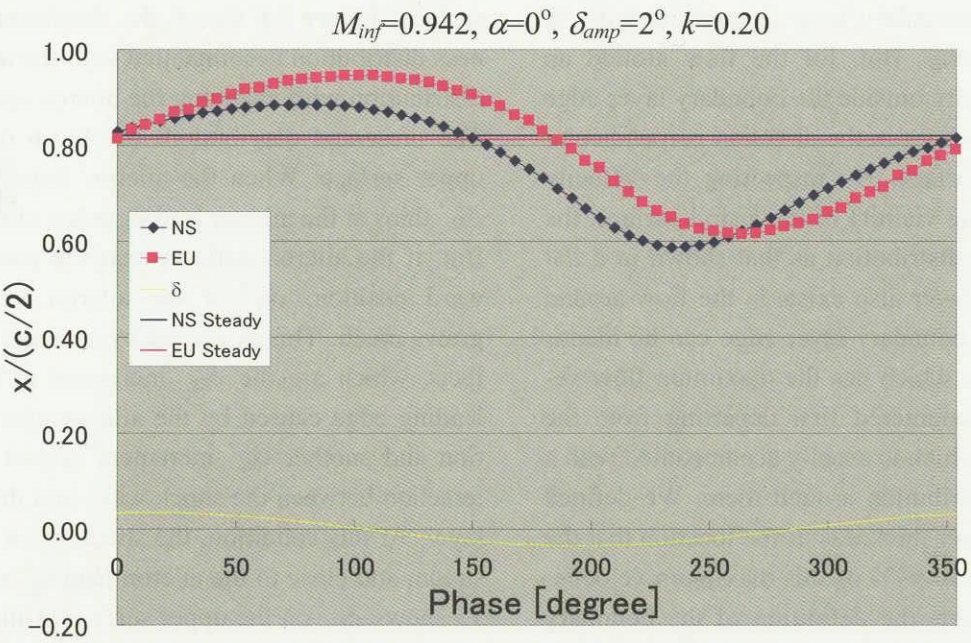

Figure 12 Comparison of Shock Wave Motion Between N-S and Euler Simulations

3.2 Mean Position of Shock Wave Motions

As clearly shown in Fig. 4(a), the shock wave oscillates around the mean position which is upstream of the steady shock wave, though this phenomenon might appear when the shock wave motion is restricted to the aileron surface. In order to inspect this characteristic, an Euler simulation is conducted to consider the viscosity effect. The simulated case is α=0°, δ_{amp}=2°, k=0.20 and M_{inf} =0.942. The reason why this case was chosen is that, when the shock wave oscillates around the aileron mid-chord with an enough extent, the unsteady flow around

the aileron representatively generates a positive Im($C_{m\delta\_u}$) value. Figure 12 shows the shock wave motions for both of the N-S and the Euler simulations. The steady shock wave for each case is also shown. The steady shock waves locate at almost the same chord position for each simulation. The shock wave oscillation is wider for the Euler simulation comparing with the N-S one. Although the unsteady shock wave still oscillates around the point upstream of the steady one, the distance between them is much less than that shown in the N-S result. This represents that the flow viscosity strongly influences on the shock wave oscillations.

As the next step, the unsteady boundary layer distributions of the simulated result are calculated for the above mentioned case. There are no explicit descriptions to define the boundary layer thickness on an airfoil. If it is on the flat plate without a pressure gradient, the velocity distribution perpendicular to the surface reaches to its 99% free-stream velocity at the boundary layer edge, and the velocity outside the boundary layer is constant with its free-steam velocity. But, for the flow around an airfoil, the velocity outside the boundary layer edge continuously changes in the direction perpendicular to the airfoil surface. By inspecting the velocity distribution in the vicinity of the airfoil surface, the similar velocity distribution as that shown in a flat plate boundary layer also exists in the flow around the airfoil. The boundary layer edge can be identified as the point which has the maximum flow velocity to be encountered first departing from the airfoil surface, which is usually accompanied with a flat velocity distribution around there. We defined the boundary layer thickness as the location that the velocity reaches to 99% of this maximum velocity. Figure 13 explains the definition of the boundary layer thickness around the airfoil. The displacement thickness, δ_{BL}^{*} is calculated as follows:

$$\delta_{BL}^{*} = \int_{0}^{\delta_{BL}} \left(1 - \frac{u}{U_{\delta_{BL}}}\right) d\eta \qquad (7)$$

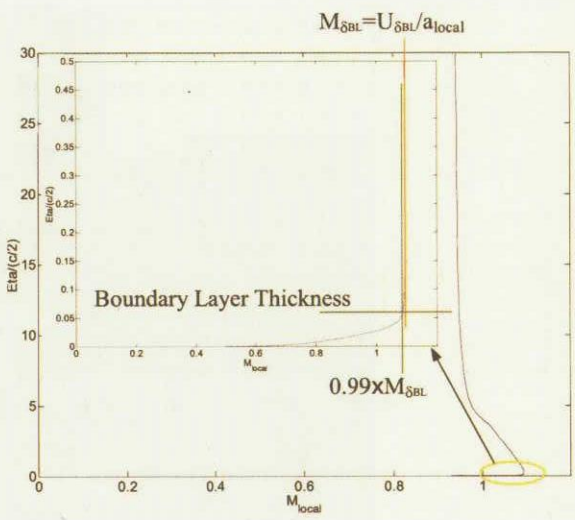

Figure 13 Boundary Layer Thickness Definition

Here, δ_{BL} is the boundary layer thickness; u is the flow velocity in the direction tangent to the airfoil surface; $U_{\delta BL}$ is the velocity at the boundary layer edge; η is the coordinate perpendicular to the airfoil surface. Figure 14 shows the displacement thickness distribution accompanied with the unsteady C_P distribution with changing the aileron motion phase. The presented distributions are those only on the upper surface. When the aileron stays downward, δ_{BL}^{*} thins at the aileron leading edge, and vise verse. But, if the aileron deflects near the maximum upward position, δ_{BL}^{*} at the aileron leading edge grows much. This is caused by a merge of two effects, which are the δ_{BL}^{*} increment at the aileron leading edge caused by the aileron upward deflection and another δ_{BL}^{*} increment caused by the interaction between the shock wave and the boundary layer. At this condition, the shock wave moves upstream and close to the aileron leading edge. Figure 15 shows δ_{BL}^{*} on the upper surface as the value averaged through one cycle. Behind the aileron leading edge, the averaged δ_{BL}^{*} is thicker than the steady δ_{BL}^{*}. In general, if an airfoil thickens, the shock wave is formed at the more upstream position. And this relation might be also applied to the averaged unsteady flow field with an increased averaged δ_{BL}^{*}.

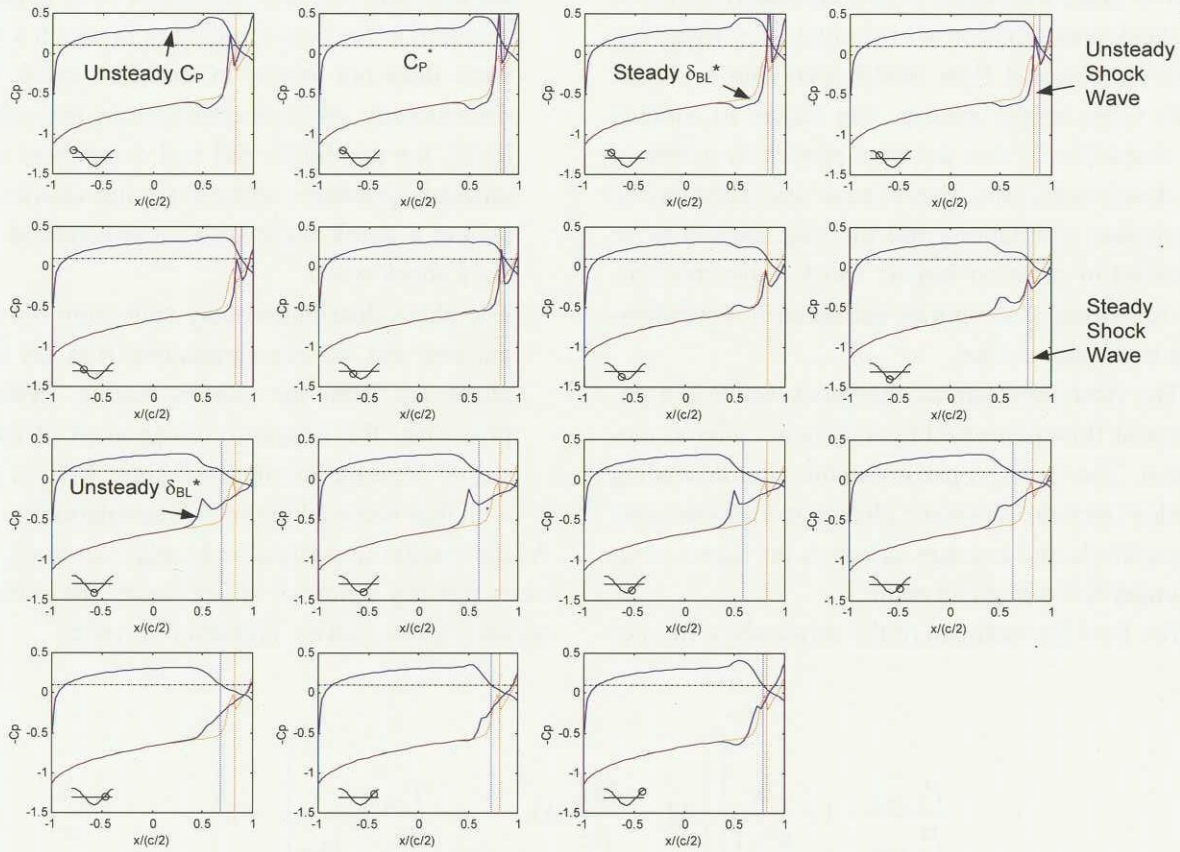

Figure 14 Time History of Displacement Thickness
(M_{inf}=0.942, α=0°, δ_{amp}=2°, k=0.20)

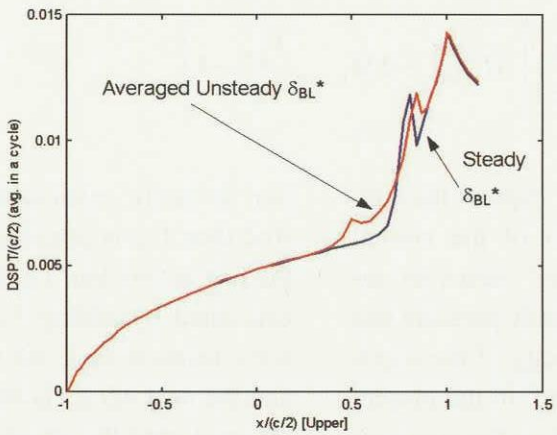

Figure 15 Steady and Averaged Unsteady Displacement Thickness

3.3 Non-Harmonic Characteristic of Shock Wave Motions

Adding to the characteristic explained in Paragraph 3.2, another one is also seen in Fig. 4, especially in Fig. 4(a).. The shock wave oscillated non-harmonically even though the aileron oscillated harmonically. That is, the shock wave stayed for a longer period in the downstream half cycle than the upstream half cycle. This characteristic is also shown in the Euler simulated result presented in Fig. 12. Therefore, the flow viscosity might not be the fundamental reason to cause this characteristic. In

order to make the reason of this characteristic clear; the shock wave motion was simulated by assuming a one-dimensional flow model involving a normal shock wave on the aileron. The reason to conduct this simulation is that the flow properties upstream and downstream of a shock wave are indecisive in the viscous simulations and they are needed to be presented in order to inspect shock wave motions. The following assumptions are taken in considerations in the simulation:

1) The flow upstream of the shock wave is a potential flow generated by a dynamic aileron motion. The flow properties at the aileron leading edge obey the harmonic change having the same amplitude and average values as the above mentioned N-S simulated result.
2) The flow downstream of the shock wave follows the unsteady pressure oscillation in its amplitude acquired in the N-S simulation, in which a shock wave does not appear in an entire cycle. From the unsteady pressure distributions presented in Ref.3, the amplitude and real component of the unsteady pressures showed similar distributions behind a shock wave with those acquired without a shock wave.

   The phase distribution may shift from the original one and, in this simulation, it is set to 45° phase lag from the aileron motion. With this phase lag, the imaginary component of the unsteady pressure distribution agrees well, in shape, with that acquired in the N-S simulation.

As the constituting equation to relate unsteady pressures passing a normal shock wave, the following equation presented by Tijdeman[9] is used:

$$\frac{P_{2\_unst}}{P_{1\_unst}} = 1+\frac{2\kappa}{\kappa+1}\left[\left\{M_1+\frac{\partial M_1}{\partial x}\Delta x-\frac{V_{SW}}{a_1+\left(\partial a_1/\partial x\right)\Delta x}\right\}^2-1\right]$$

$$=1+\frac{2\kappa}{\kappa+1}\left[\left\{M_{1\_unst}-\frac{V_{SW}}{a_1}\right\}^2-1\right]$$

$$\cong 1+\frac{2\kappa}{\kappa+1}\left[M_{1\_unst}^2-2M_{1\_unst}\frac{V_{SW}}{a_1}-1\right] \qquad (8)$$

Here, the subscriptions '*1*' and '*2*' express the conditions upstream and downstream of the normal shock wave. The subscription '*unst*' means an unsteady value. P and M are the unsteady pressure and the Mach number. V_{SW} is the velocity of the shock wave motion. a is a speed of sound. In the present simulation, a_1 is assumed constant on the entire aileron surface as the value just behind the aileron leading edge. And V_{SW}/a_1 is assumed to be small enough comparing to M_{1_unst}.

At the first step, the unsteady shock wave position is assumed to be equal to the steady shock wave position. The pressure ratio distribution across the shock wave is given from the above assumptions 1) and 2) at every time step. M_{1_unst} at the certain position is easily calculated from the assumption 1). And then V_{SW} is calculated from the equation (8) as the first estimation. The next shock wave position is calculated by adding $V_{SW}\Delta t$ to the previous shock wave location, Δt is the time step in the simulation, and the next M_{1_unst} is calculated. This procedure is repeated until the simulation converges. The simulated shock wave motion is shown in Fig. 16 accompanied with the time-histories of other flow properties. Although the shock wave seems to oscillate downstream of the N-S result, the non-harmonic shock wave motion was acquired in this simulation. The shock wave stays for a longer period in the downstream half cycle, 55% of a cycle, than the upstream half cycle. The reason to cause

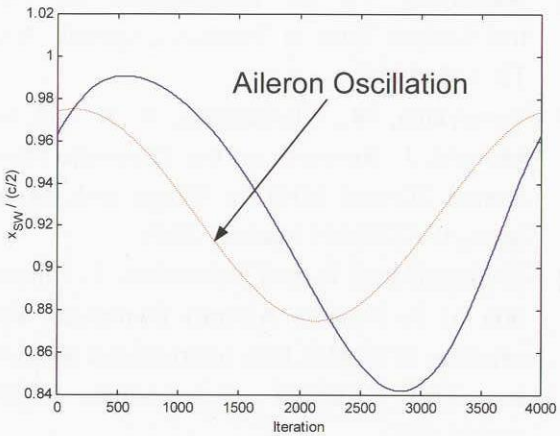

(a) Shock Wave Location

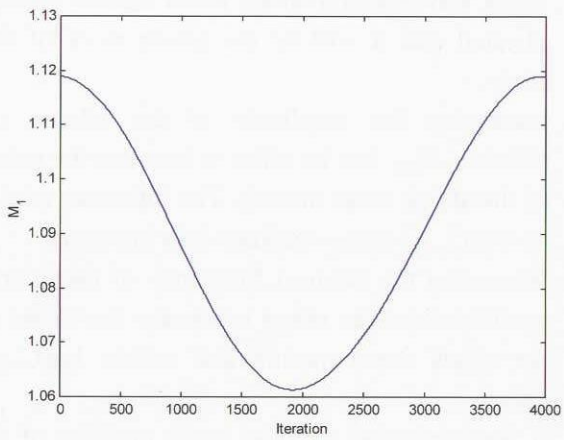

(b) Mach Number Upstream of Shock Wave

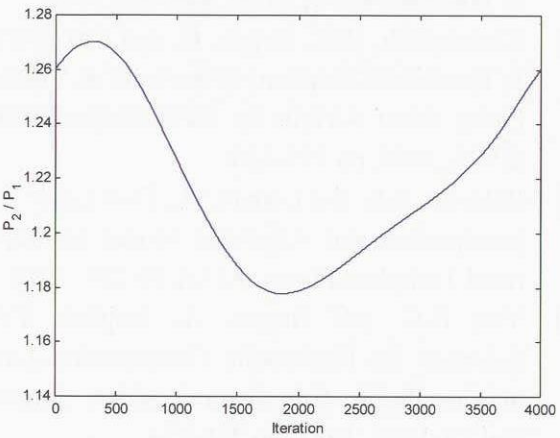

(c) Pressure Ratio Across Shock Wave

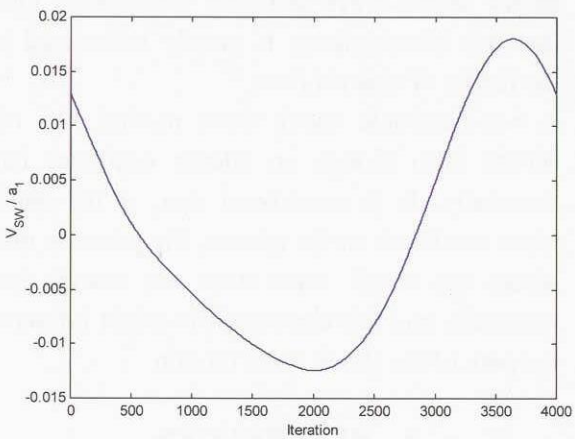

(d) Speed of Shock Wave Motion

Figure 16 Properties Acquired From One-Dimensional Simulation of Shock Wave Motion

the non-harmonic shock wave motion can be explained by the presence of the non-harmonic change of the pressure ratio as shown in Fig. 16. Considering from this characteristic of the shock wave motion, when the shock wave exists on an aileron, it must be taken care that equations are not easily simplified by assuming a harmonic shock wave motion.

4 CONCLUSIONS

In order to acquire the relations between the shock wave motion and the aileron hinge moment around a thin airfoil with an aileron, unsteady N-S simulations were conducted on a two-dimensional NACA0003 airfoil with an oscillating 25% chord-length aileron. In the simulations, some parameters were varied. From this study, the followings are summarized as the conclusions:

1. A Shock wave oscillates on the upper surface continuously. On the other hand, that on the lower surface oscillates intermittent.
2. For each α case, the mean location of the shock wave motion changes linearly against the free-stream Mach number on the upper surface unless the shock wave reaches the airfoil trailing edge.
3. The shock wave oscillates narrower as α increases if it oscillates around the same mean position.
4. The reachable level of the imaginary component of the unsteady pressure coefficient, $\mathrm{Im}(C_{m\delta\_u})$, decreases as α increases. The shock wave appearance on the lower surface might influences on this tendency. The categorization of the

shock wave motion on the lower surface is complicated and it will be the future work of this study.

5. Increasing the amplitude of the aileron oscillation, δ_{amp}, has an effect to broaden the extent of the shock wave motion. The influence of δ_{amp} on $\mathrm{Im}(C_{m\delta\_u})$ value weakens as α increases.
6. Increasing the reduced frequency of the aileron oscillation has an effect to narrow the extent of the shock wave motion and reduce $\mathrm{Im}(C_{m\delta\_u})$ value.
7. It was observed that the mean position of the shock wave motion is inconsistent with the steady shock wave position. It becomes clear that this inconsistency is greatly influenced by the nature of viscous flow.
8. A non-harmonic shock wave motion was observed even though an aileron oscillates harmonically. It is considered that, if the shock wave oscillates on the aileron, the pressure ratio across the shock wave dose not change harmonically and this characteristic might influence the path of the shock wave motion.

5 REFERENCES

[1] Lambourne, N.C., Control-Surface Buzz, Aeronautical Research Council R.&M. No.3364, 1964.

[2] Nakamura, Y., An Investigation on Control-Surface Buzz at Transonic Speeds, NAL TR-155, 1968.

[3] Tamayama, M., Kheirandish, H. R. and Nakamichi, J., Research on the Transonic Flows around 2D and 3D Thin Wings with an Aileron, IFASD2001 Madrid, 2001.

[4] Kheirandish, H.R. and Nakamichi, J., Simulation of A Flexible Aircraft Dynamics, Proceedings of JSASS 13th International Sessions in 37th Aircraft Symposium, 1999, pp.665-668.

[5] Bendiksen, O.O., Nonclassical Aileron Buzz in Transonic Flow, AIAA 93-1479, 1993.

[6] Kheirandish, H.R., Beppu, G. and Nakamichi, J., Numerical Solutions of Inviscid & Viscous Flows about Airfoils by TVD Method, NAL SP-27, 1994, pp.135-140.

[7] Baldwin, B.S. and Lomax, H., Thin Layer Approximation and Algebraic Model for Separated Turbulent Flows, AIAA 78-257, 1978.

[8] Yee, H.C. and Harten, A., Implicit TVD Schemes for Hyperbolic Conservation Laws in Curvilinear Coordinates, AIAA Journal, Vol.25, No.2, 1987, pp.266-274.

[9] Tijdeman, H., Investigations of the Transonic Flow Around Oscillating Airfoils, NLR TR 77090 U, 1977.

JAXA Research and Development Report
(JAXA-RR-03-017E)

Date of Issue : March 25, 2004

Edited and Published by :
Japan Aerospace Exploration Agency
7-44-1 Jindaiji-higashimachi, Chofu-shi,
Tokyo 182-8522 Japan

Printed by :
BCC Co., Ltd.
2-4-1 Hamamatsu-cho, Minato-ku, Tokyo 105-6114 Japan

JAXA

Japan Aerospace Exploration Agency